Improved Plutonium Identification and Characterization Results with a NaI(Tl) Detector using ASEDRA

R. Detwiler , G. Sjoden , J. Baciak , E. LaVigne

FINDS/Nuclear and Radiological Engineering (NRE) Department
University of Florida, 202 NSB, POB 118300, Gainesville, FL 32611-8300

ABSTRACT

The ASEDRA algorithm (Advanced Synthetically Enhanced Detector Resolution Algorithm) is a tool developed at the University of Florida to synthetically enhance the resolved photopeaks derived from a characteristically poor resolution spectra collected at room temperature from scintillator crystal-photomultiplier detector, such as a NaI(Tl) system. This work reports on analysis of a side-by-side test comparing the identification capabilities of ASEDRA applied to a NaI(Tl) detector with HPGe results for a Plutonium Beryllium (PuBe) source containing approximately 47 year old weapons-grade plutonium (WGPu), a test case of real-world interest with a complex spectra including plutonium isotopes and ^{241}Am decay products. The analysis included a comparison of photopeaks identified and photopeak energies between the ASEDRA and HPGe detector systems, and the known energies of the plutonium isotopes. ASEDRA's performance in peak area accuracy, also important in isotope identification as well as plutonium quality and age determination, was evaluated for key energy lines by comparing the observed relative ratios of peak areas, adjusted for efficiency and attenuation due to source shielding, to the predicted ratios from known energy line branching and source isotopics. The results show that ASEDRA has identified over 20 lines also found by the HPGe and directly correlated to WGPu energies.

Keywords: Pu-239, WGPu, spectroscopy, isotope identification, radiation detection, NaI, HPGe, Homeland Security

1. INTRODUCTION

Researchers at the Florida Institute of Nuclear Detection and Security (FINDS) in the University of Florida's Nuclear and Radiological Engineering Department have developed a unique algorithm that post-processes scintillator detector spectra to render photopeaks with high accuracy. The post-processed spectrum output is directly comparable with resolved spectra from high resolution semiconductor detectors. The algorithm, ASEDRA (US Patent 60/971,770; 9/12/2007), stands for "Advanced Synthetically Enhanced Detector Resolution Algorithm." ASEDRA[1] is currently applied to sodium iodide (NaI(Tl)) detectors, which are highly robust but, until now, had limited identification capabilities due to poor energy resolution. By rapidly post- processing a NaI(Tl) detector signal with ASEDRA over a few seconds on a standard laptop, and with no prior knowledge of sources or specific spectrum features, gamma ray lines are extracted on a level directly competitive with nitrogen cooled germanium detectors. ASEDRA incorporates a novel denoising algorithm based on an adaptive Chi-square metric called ACHIP (also under USP 60/971,770), to remove stochastic noise from low count spectra yet preserve fine detail, then employs a novel detector response algorithm to reveal specific gamma lines that composed the gamma ray spectrum.

2. METHODOLOGY

2.1 The Experimental Goal

The work reported on here involves testing of the ASEDRA algorithm performance on NaI spectra taken with a PuBe source containing 16g of shielded WGPu. A separate paper [2] reports on testing of ASEDRA with other gamma sources, including ^{137}Cs, ^{133}Ba and ^{152}Eu. The primary purpose of the WGPu data comparisons was to test ASEDRA's performance with a spectrally challenging source of real-world interest, as well as verifying ASEDRA's limits of performance for low statistics spectra, and shielded source spectra. Testing involved spectra processed with ASEDRA

using standard settings to verify applications for field use. However, the experimental verification tests also included determining ASEDRA's utmost abilities, such as the case of the 10 minute WGPu spectra, along with investigation of the effects of parameter changes in algorithm settings, as well as dependence on energy and FWHM calibrations.

2.2 PuBe Source and Experimental Setup

The source used during these tests was a PuBe Source containing WGPu which was approximately 47 years old, with an isotopic enrichment of 93.54% ^{239}Pu. The source geometry is shown in Figure 1 shown below; the source dimensions were approximately 2.57 cm outside diameter x 3.68 cm long, with an outer stainless steel cladding layer of 0.25cm thick over an inside Ta cladding layer 0.25 cm thick. The diameter of the PuBe region inside the two cladding layers was 1.58 cm. Source spectra for both detectors verified the ^{241}Am content of approximately 1 % by weight with what had been assumed from a previous source characterization [3] using HPGe ratios for the 662.4keV ^{241}Am line relative to key WGPu lines. Table 1 shows ^{241}Am and ^{239}Pu lines used in the experimental verification. The analysis identified other Pu isotopes as well as ^{241}Am, a decay product. Comparison HPGe spectra were taken for all source configurations. The ASEDRA NaI photopeak energies are compared to photopeak energies from HPGe spectra and to known WGPu and decay product energies [4, 5].

Side by side comparisons were conducted with the HPGe and NaI detectors; all runs were taken with the source at 1 m from the detectors. Spectra were taken for both the non-shielded PuBe source, and for the source in a composite metal shield of greater than 5 MFP for the given photon energies. Comparisons included both high statistics spectra such as 10 minute spectra with the unshielded source configuration, as well as low statistics tests such as the shielded source runs and 1 minute of counting. HPGe comparison spectra served a dual purpose; both to provide reference spectra for verification of energy lines identified by ASEDRA, and also to provide a high resolution standard for nuclide identification as a comparison for ASEDRA's NaI peak analysis results.
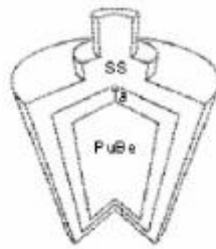

Fig. 2. PuBe Source Geometry showing interior WGPu source with Stainless Steel and Ta Cladding layers

2.3 Photopeak Energy Analysis

The spectral analysis was conducted on background-subtracted spectra for both the HPGe and NaI detectors. ASEDRA was used to analyze the NaI spectra, while GENIE2K was used to analyze the HPGe spectra to provide a comparison of ASEDRA's capabilities with NaI to that of a typical HPGe detector with off-the-shelf (OTS) HPGe peak identification software. However, several HPGe peaks not found by this OTS software were visually identified and are listed in Table 1. To provide a fair comparison, results for the standard settings and thresholds were used for both software for the higher count spectra; when lower thresholds improved results for ASEDRA, results were included (indicated with an *) for a lower threshold with the HPGe and GENIE2K software.

All photopeaks identified are compared to known photon or x-ray energies from WGPu, or from other known contaminants, with branching ratios shown for photon energies [5,6]. Raw experimental photopeak counts not corrected for attenuation or detector efficiency are also shown for each photopeak energy identified.

2.4 Photopeak Yield Analysis

A comparison of relative photopeak yields to predictions was also conducted using branching ratios for gamma decay [5]. The analyzed photopeak yields were corrected for detector efficiencies; the relative detector efficiencies were

measured as a function of photon energy using the same experimental electronics and physical setup of detectors. Due to the shielding of the source geometry, select prominent Pu lines close in energy were compared for relative yields, to minimize errors due to attenuation estimations. The source shielding corrections were both hand calculated using linear interpolation of attenuation coefficients to specific energies [6], as well the photo-peak attenuation was modeled using Monte Carlo simulation (MCNP5) for the PuBe source geometry.

Table. 1. Estimate of [241]Am content from spectral data and comparison to predicted value assuming 47 year old WGPu [3].

Am-241 Enrichment Calculation				
E(keV)	Counts Yield-Corr	Calc. weight ratio	Ave. Meas. Weight Ratio	Predicted[3] Mass Ratio
			[662, 722]	
662/413	4.63E-01	8.36E-03		
722/413	6.69E-01	1.21E-02	1.02E-02	0.008
208/202	1.27E+00	2.29E-02		

3. SPECTRA

3.1 Comparison of High Statistics Spectra

Sample spectra are shown in this section. For unshielded WGPu source, comparison HPGe and NaI spectra were taken at 10 minute, 5 minute, and 1 minute lengths (NaI spectra were also taken for 3 minutes). Figures 2 and 3 show, respectively, the full energy (~ 3 MeV) 10 minute spectra taken with the HPGe and NaI detectors. Key energy lines shown in the analysis are identified; it is important to note that while ASEDRA did identify the 2223 keV line (to within 1%), the Genie2K analysis with the HPGe did not. However, the line was visually identified. Also shown in the HPGe spectra are known gammas from (n,n') and (n,γ) reactions on Ge. Figures 4 and 5 show respectively the lower 800 keV energy windows of these spectra due to the numerous Pu photopeaks in this region. The NaI spectrum with ASEDRA analysis shows nearly all Pu lines identified by the HPGe in this region; however several photopeaks close in energy do appear as a convoluted peak for NaI. The 332 and 336 keV lines appear as part of the 344 keV line, and the strong 375 keV line includes the weaker 380 and 382 keV lines. The energies shown in these figures are the known energies; Tables 1 and 2 show a break-down of ASEDRA and HPGe identified photopeak energies vs. known photopeak energies.
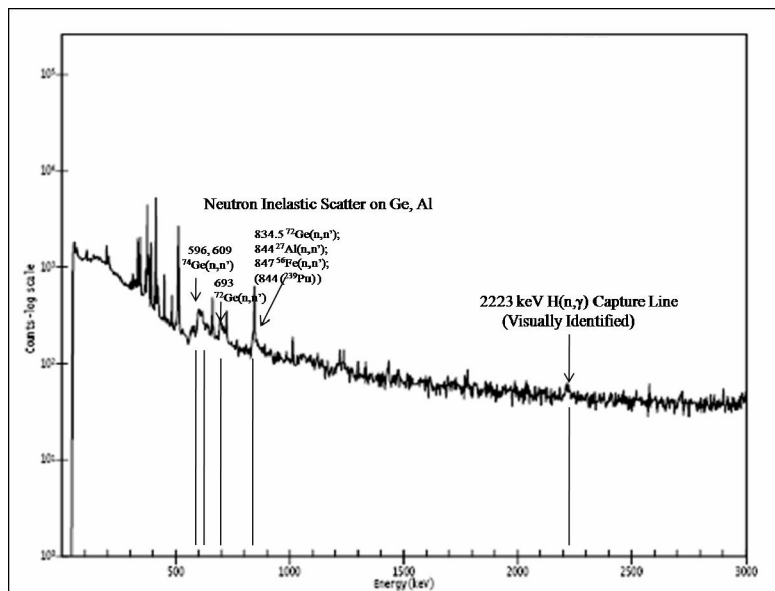

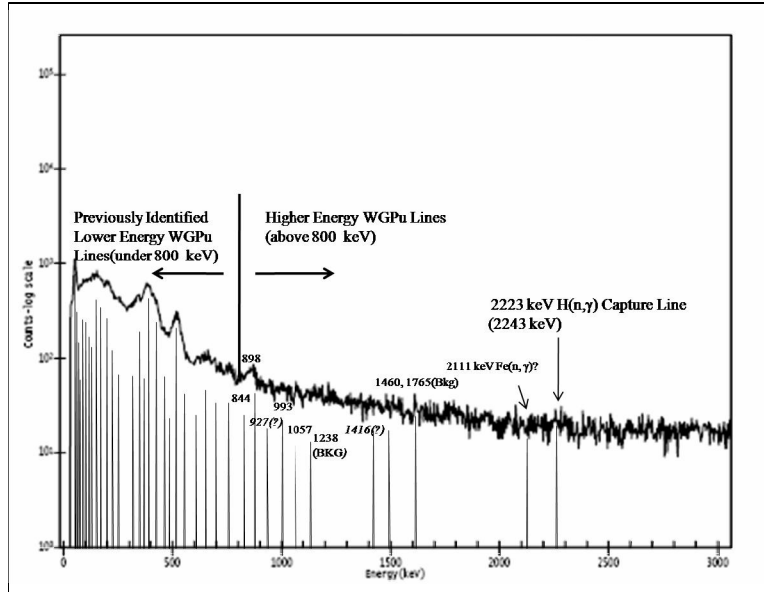Fig. 2. HPGe 800 keV Spectrum; WGPu lines as well as neutron activation lines from Ge are shown.

Fig. 3. ASEDRA shows identification of all WGPu lines found by HPGe. ASEDRA identifies major WGPu/Am lines (344, 375, 414, 59.5, 662 keV). Energies are within 1% for almost all WGPu peaks identified.
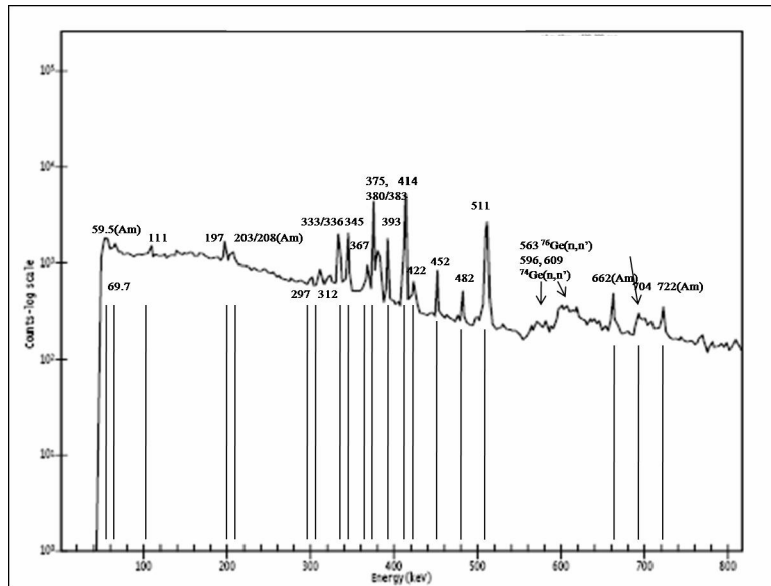

Fig. 4. HPGe 800 keV Spectrum; WGPu lines as well as neutron activation lines from Ge are shown.
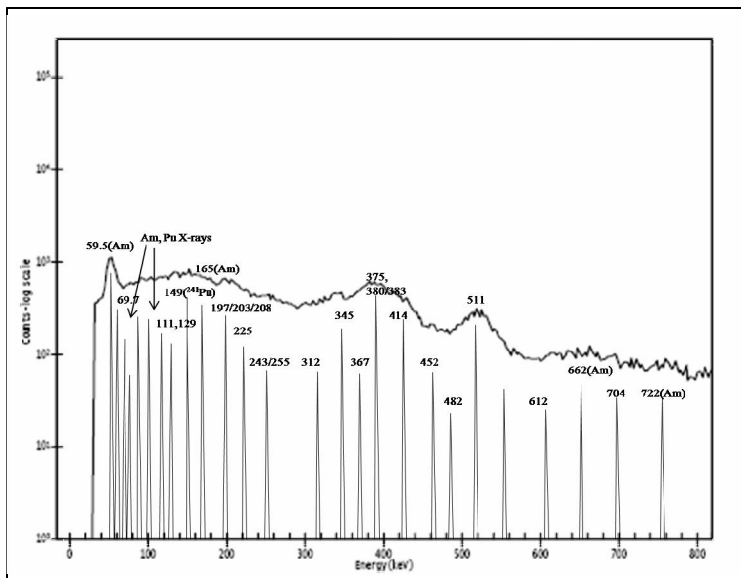
Fig. 5. ASEDRA shows identification of all lower energy WGPu lines found by HPGe. ASEDRA identifies major WGPu/Am lines (344, 375, 414, 59.5, 662 keV) to within 1% of known values for most peaks.

3.2 Spectra with Lower Statistics

NaI and HPGe spectra were also taken for the WGPu source encased in a cylindrical composite metal shield[3]. Table 2. gives the full data set, including ASEDRA results for 10, 5 and 1 minute NaI spectra, and identified peaks from a reference 10 minute HPGe spectra. Shown below in Figures 6 and 7 are 1 minute NaI spectra with some key ASEDRA peaks shown (the full peak list is in Table 2.) and key lines from the 10 minute HPGe spectra (Figure 8). Although the shield material composition is patent-pending, three photopeaks observed in the HPGe spectra (1332, 1434, 1454 keV) are known gamma energies from (n,γ) reactions with the shield, and the prominent x-ray at 69 keV is also from this shield. These photopeaks were also observed in the ASEDRA / NaI results; the 1 minute NaI spectra shows a strong 69 keV x-ray peak and identified peaks at 1327 keV and 1427 keV which clearly correspond (with a small energy uncertainty) to these contaminant lines. Also important is the identification by ASEDRA of the 2223 keV photopeak in this 1 minute spectra, shown in Figure 7.
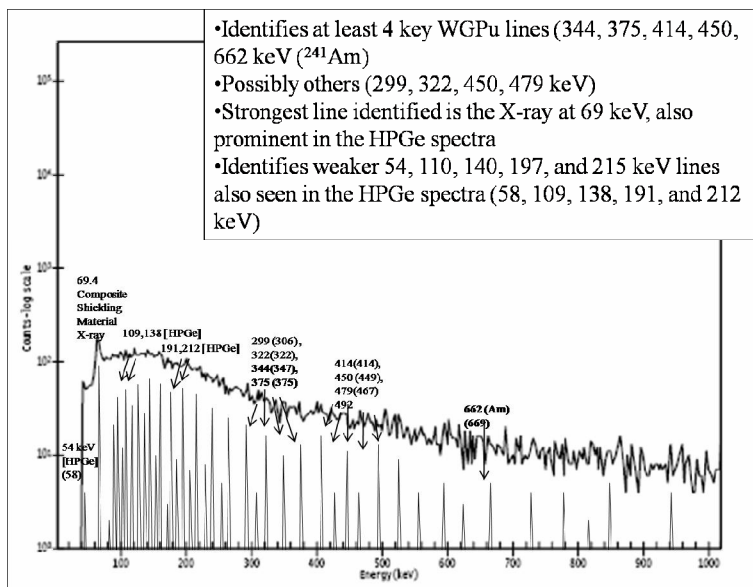

Fig. 6. ASEDRA results with key WGPu lines for a 1 minute NaI spectra with composite metal shield.
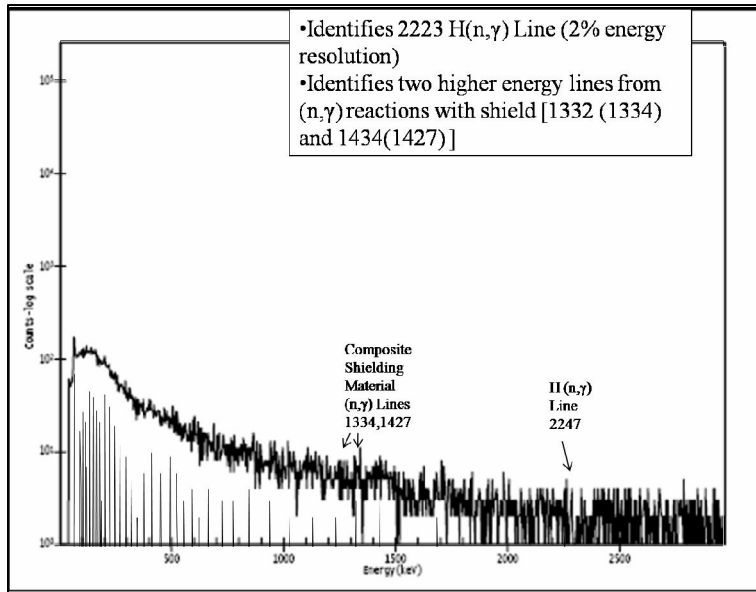
Fig. 7. ASEDRA identification of higher energy lines for a 1 minute NaI spectra with a composite metal shield.
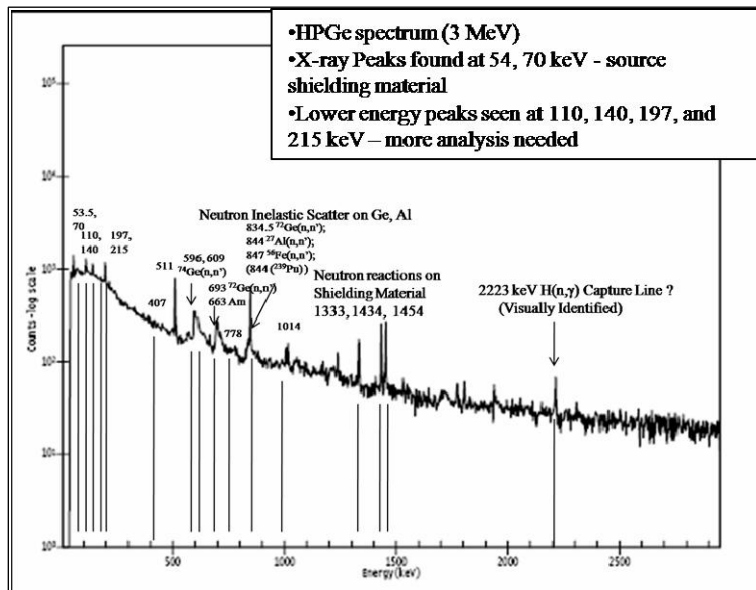

Fig. 8. HPGe 10 minute spectra with a composite metal shield and key WGPu lines identified.

4. RESULTS

4.1 High Statistics Photopeak Energy Comparisons

The results of the analysis are shown in the following tables below; Table 1 shows the higher count WGPu spectral results taken, showing photopeaks identified with energies and counts for HPGe and NaI detectors Photopeak experimental energies are shown compared to reference energies [5, 6]. NaI-ASEDRA data are compared to HPGe data for the 10 minute and 5 minute runs. No HPGe run was taken for under 3 minutes; however an NaI spectrum is shown.

As mentioned above, the HPGe spectra photopeak energies and photopeak counts were obtained by the GENIE2K software, as well as visual identification, while peak fitting for the NaI spectra was conducted with ASEDRA. For the 10 minute runs, a higher minimum threshold proved optimal for both for the HPGe and ASEDRA/NaI analysis for the 10 minute spectra; for the 5 minute and 3 minute NaI runs, a lower threshold was used for ASEDRA. For these tests, both a standard (3 sigma) and lower (2 sigma) threshold were used with Genie2K for the HPGe 5 minute run; also for this HPGe run, * indicates that the identified photopeak energy was present for the lower threshold.

4.2 Low Statistics Photopeak Energy Comparisons

Table 2. shows the lower statistics spectral results for HPGe and NaI detectors obtained with the PuBe source in the shielded configuration.   Here, the HPGe photopeaks identified are again displayed with two thresholds, * indicating the lower 2-sigma threshold; while the lower threshold does provide more WGPu known lines, there are also considerably more false positives. The ASEDRA results for the longer 10 minute, 5 minute and 3 minute runs are shown for standard thresholds; at this threshold the 2223 MeV $H(n,\gamma)$ is identified in the 10 minute and 5 minute spectra, and several key Pu lines (344, 375, 414 keV) are identified to within 1-2% accuracy.

The 1 minute NaI spectrum was analyzed by ASEDRA with a lower threshold. At least 4 key Pu lines (344, 375, 414, 450 keV) are identified to within 1 - 2%. In addition, the strong 69 keV x-ray from the composite material is identified as the strongest peak by ASEDRA, and 1333 and 1434 keV (n,γ) peaks from the composite shielding material indicated by ** are also identified.   There are also roughly 10 weaker photopeaks which may correspond to peaks identified in the longer statistics runs. These are also shown in Table 2, although their statistics are low.

4.3 Photopeak Yield Comparisons

Table 1 shows relative yield comparisons for ASEDRA NaI analysis results with standard thresholds and settings to predicted and measured HPGe relative yields. Due to the shielding of the source, both from the Ta and Stainless Steel cladding layers, and from the source self-shielding, the yield comparison was done for the strongest photopeaks in the 300 keV – 400 keV region to minimize error from attenuation; yields of lower energy lines were not compared due to the higher error in shielding corrections. However, the compared yields for key energy lines include corrections for attenuation due to the shielding. Corrections using attenuation coefficients from [5] are shown, and have an approximately 10% error in attenuation correction due to extrapolation. Yield comparisons to predictions obtained from MCNP transport calculations for these energies with the given source geometry are also shown.

To further minimize experimental and attenuation correction error, relative yields are compared to expected values. The yields are normalized to the strongest [239]Pu lines at 375 keV and 414 keV; values shown are the ratio of measured to predicted normalized yields. The 344 keV peak includes contributions from the 332/336 keV peaks, while the 375 keV peak includes the contributions of the weaker 380 and 382 keV peaks. In addition to the [239]Pu lines, the relative yields of the higher energy [241]Am lines (722 keV to 622 keV) are shown (the value is again the ratio of the measured to expected relative yield). The stronger [241]Am 662 keV yield normalized to the 375 keV and 414 keV [239]Pu lines is also shown; however this value has error associated with the estimate of the age of the source and [241]Am content.

Table. 1. Higher Count WGPu Spectral Results

Known Energy	Yield	Isotope	10 Min HPGe (E)	10 Min HPGe(Cts)	10 Min NaI(E)	10 Min NaI(Cts)	5 Min HPGe (E)	5 Min HPGe(Cts)	5 Min NaI(E)	5 Min NaI(Cts)	3 Min NaI(E)	3 Min NaI(Cts)
59.5	35.9	Am-241	54.18	1140	58.33	933.92	54.19	6.10E+02	58.33	455.39	58.33	223.59
67.4	K-edge	Ta X-ray	65.42	194	65.60	235.11	65.51	2.50E+02	65.60	140.16	65.60	100.88
75	K-shell	Pb X-ray*			74.33	320.58			72.88	87.85	71.42	35.35
88	K-edge	Pb X-ray*			85.97	281.74			83.06	138.49	80.15	84.78
99.7	K-shell	Pu X-ray			91.79	130.80			93.25	126.15	91.79	99.61
104	K-shell	Pu X-Ray			100.52	357.83			99.07	27.49	100.52	66.79
116	K-shell	Pu X-Ray	109.33	496	110.71	245.93	109.73	2.91E+02	106.34	167.06	110.71	117.70
121.00	K-edge	Pu X-Ray			122.37	429.63			116.53	118.52	119.44	51.65
129.3	6.31E-03	Pu-239			132.96	223.75			128.42	201.54	128.42	144.16
141.6	3.20E-05	Pu-239	138.89	160					137.50	62.10	137.50	67.79
148.6		Pu-241			145.06	596.32			146.58	260.34	148.09	174.84
									155.65	83.85		
164.3, 169.5	6.67E-5, 17.3E-5	Am-241			166.24	524.35			167.76	301.70	164.73	146.19
179, 189	1.10E-04	Pu-239			182.88	208.16			179.86	58.90	181.37	114.81
195.7	1.11E-03	Pu-239	197.22	986			197.1	5.71E+02	191.96	253.71	191.96	28.39
203.5	5.69E-04	Pu-239	202.91	306	201.04	508.19	*203.21	2.13E+02			204.06	122.90
208.0	7.91E-04	Am-241	207.98	539			*207.29	2.16E+02	210.12	204.56	216.17	26.23
225.4	1.51E-05	Pu-239			228.27	335.05			225.24	89.49	228.27	109.48
243.4	3.77E-05	Pu-239							241.89	152.92	241.89	15.08
255.4	8.00E-05	Pu-239			261.45	273.04			256.94	28.74	253.93	93.58
267.5	2.63E-05	Am-241							268.97	129.77	270.48	14.25
											281.00	81.29
297.5	2.58E-05	Pu-239	301.78	164	285.51	97.79	*297.6	5.49E+01	293.03	87.51	299.05	32.17
311.7	5.90E-05	Pu-239	312.03	524	309.58	262.40	311.34	8.33E+01	318.60	164.63	315.59	91.93
320.9	6.06E-04	Pu-239	322				332.24	4.15E+01				
332.8*	1.12E-04	Pu-239	332.2	337			335.28	6.46E+00			330.63	24.84
336.113*	6.06E-04	Pu-239	335									
345.0	6.06E-04	Pu-239	345.02	1852	344.16	421.82	345.02	9.60E+02	350.43	217.28	348.86	116.71
350.8	1.80E-06	Pu-239	351.97	visually								
367.0	1.77E-04	Pu-239	367.41	570	366.11	95.46	368.28	3.66E+02	367.68	74.91	366.11	37.21
375.0	1.55E-03	Pu-239	374.93	6297	384.93	641.70	374.94	3.10E+02	388.06	362.50	384.93	156.94
380.2	3.05E-04	Pu-239	380.24	772	Included		380.16	4.12E+02	Included			
382.8	2.59E-04	Pu-239	382.62	521	" "		382.58	2.53E+02	" "			
393	5.98E-04	Pu-239	392.94	2647	" "		392.66	9.20E+02	" "			
413.713	1.47E-03	Pu-239	413.58	6785	419.43	401.42	413.57	3.35E+03	419.43	205.37	414.72	109.85
422.6	1.22E-04	Pu-239	422.79				451.43	5.08E+02				
451.5	1.89E-04	Pu-239	451.4	926	452.35	142.24			449.22	84.12	444.51	53.09
481.7	4.60E-06	Pu-239	482.05	443	486.85	79.57	482.07	2.55E+02	483.72	47.21	483.72	36.60
511.0			510.85	5936	518.22	243.65	510.82	2.90E+03	516.65	123.97	521.36	63.26
545/558		Ge(n,n')			551.17	69.51	*529.66	1.87E+01	540.18	45.81	562.15	29.37
612.83	9.50E-07	Pu-239	609.05	visually	618.63	48.44	*545.9	5.79E+01	569.99	15.08		
							*596.74	7.86E+01	604.51	28.25		
645.9	1.52E-05	Pu-239							640.60	19.90	621.77	14.83
662	3.64E-04	Am-241	662.22	513	665.73	77.14	662.46	2.32E+02	668.89	41.90	668.89	34.24
703.7	4.95E-06	Pu-239	693.62	138	698.92	42.18			703.66	21.38		
722.0	1.96E-04	Am-241	722.09	368								
756.4	3.47E-06	Pu-239			747.91	52.86	722.22	1.29E+02	747.91	30.58	740.01	18.26
808.4	1.21E-07	Pu-239			804.81	35.42	*794.15	5.11E+01	792.16	21.87	804.81	11.81
843.78	1.34E-07	Pu-239	846.6	1009	864.86	47.91	846.52	5.07E+02	864.86	24.12	869.60	16.64
898.1	1.80E-08	Pu-239							907.53	11.98		
957.6	2.70E-08	Pu-239			943.88	31.53					929.66	12.05
992.7	3.20E-08	Pu-239							984.97	12.01	996.03	13.44
1057.3	4.50E-08	Pu-239			1016.60	33.62	*1280.61	4.79E+00	1252.50	19.95	1062.40	9.54
		(n,γ)?			1117.70	31.25	*1294.47	6.05E+00	1305.20	13.81	1117.70	8.81
		(n,γ)?			1270.00	24.68	*1298.15	2.79E+01	1359.30	11.11		
		Ge(n,n')	1332	23.7			*1421.01	1.22E+01	1419.80	14.70	1442.80	7.86
							*1552.56	2.70E-01	1514.80	21.31	1545.40	7.93
							*1726.53	4.45E+00				
							*1735.11	9.85E+00				
							*1740.91	3.49E+01				
							*1961.71	3.60E+01				
		Fe(n,γ)?			1615.90	25.29	*2059.56	5.05E+00	2072.30	11.67	1641.90	11.79
		Fe(n,γ)?			1733.80	23.91	*2095.2	3.41E+01	2156.60	12.75	1755.30	7.82
2243		H(n,γ)	2220	visually	2225.50	22.34			2225.50	11.22	2211.70	7.99
			2903.71	2.14E+01								

Table. 2. Shielded WGPu spectral results; NaI, HPGe photopeaks identified with energies and counts

			Standard Threshold								Lower Threshold	
Known Energy	Yield	Isotope	10 Min HPGe(E)	10 Min HPGe(Cts)	10 Min NaI(E)	10 Min NaI(Cts)	5 Min NaI(E)	5 Min NaI(Cts)	3 Min NaI(E)	3 Min NaI(Cts)	1 Min NaI(E)	1 Min NaI(Cts)
59.5	35.9	Am-241	53.52	7.05E+02								
69	K-edge	X-ray**	69.89; *66.21, *70.52	109; 14.4, 118	68.70	756.55	68.70	376.15	68.70	210.61	69.44	70.84
75	K-shell	X-ray	*87.1	1.44E+01	80.61	97.11	89.00	169.97	87.54	99.36	84.61	17.78
88	K-edge	X-ray	*92.52	1.18E+00	90.46	315.49					89.00	4.09
99.7	K-shell	Pu X-ray			102.17	275.28	100.71	146.32	100.71	88.16	97.78	27.79
104	K-shell	Pu X-Ray	110.1	5.72E+02	110.95	144.25	110.95	101.08	110.95	51.45	108.02	21.17
116	K-shell	Pu X-Ray									115.34	7.17
121, 129.3	K-edge, 6.31e-	Pu X-Ray			125.72	453.14	128.76	237.20	125.72	143.03	128.76	45.77
141.6	3.20E-05	Pu-239	139.89	2.63E+02	140.90	390.32	143.93	204.01	140.90	124.91	143.93	39.47
148.6		Pu-241			157.58	304.30	159.10	156.15	156.07	95.00	159.10	28.66
179.0	1.10E-04	Pu-239			174.27	227.71	175.79	125.06	169.72	62.48	175.79	21.64
189.0		Pu-239			184.89	58.81			189.45	142.78	183.38	3.11
195.7	1.11E-03	Pu-239	197.01	1.09E+03	198.55	475.45	200.07	243.36			198.55	42.81
203.5/208	5.7e-4,7.9e-4	Pu-239	215.94	3.13E+01	218.27	303.34	219.79	154.57	210.69	115.03	219.79	31.30
225.4	1.51E-05	Pu-239	*227.87	7.06E+01					231.93	70.57		
243.4	3.77E-05	Pu-239			241.03	206.45	242.55	105.33	253.17	51.69	244.06	19.19
267.5	2.63E-05	Am-241			263.81	141.84	266.84	76.71	277.47	32.79	268.36	12.83
297.5	2.58E-05	Pu-239			288.11	88.20	294.18	51.88			295.70	9.27
311.7/321	5.9e-5/6.6e-4	Pu-239	*320.54	4.15E+01	321.52	65.56	321.52	38.27	306.33	26.10	321.52	5.20
332.8/336	1.1e-5/6.1e-4	Pu-239	*327.58	1.38E+02					335.19	18.20		
345.0	6.06E-04	Pu-239			348.97	41.16	348.97	25.46			347.42	2.52
375.0	1.55E-03	Pu-239	*389.58	8.88E+00	377.01	72.20	377.01	42.30	386.36	24.49	378.57	6.34
393	5.98E-04	Pu-239	*395.9	8.61E+01	398.82	35.28	398.82	18.37				
413.713	1.47E-03	Pu-239	407		425.31	76.23	420.63	49.70			414.40	10.30
422.6	1.22E-04	Pu-239	*419	7.25E+01					423.75	29.80		
451.5	1.89E-04	Pu-239			458.02	61.30	456.46	40.97	459.58	24.97	454.90	6.27
481.7	4.60E-06	Pu-239			496.96	107.65	500.08	56.96	501.64	37.43	498.52	9.92
511.0		Pu-239	510.89	1.65E+03	531.09	55.54	532.64	29.97	535.73	19.61	528.00	6.90
545/558		Ge(n,n')			577.50	45.00	572.86	20.29	566.67	11.97	558.94	3.13
612.83	9.50E-07	Pu-239	595.64	9.39E+01	609.99	26.42			602.25	18.20	597.61	4.32
							625.45	27.39			627.00	2.15
645.9	1.52E-05	Pu-239			640.92	51.99	680.01	21.61				
662	3.64E-04	Am-241	663.02	1.82E+01	680.01	37.66			668.93	19.76	668.93	4.39
703.7	4.95E-06	Pu-239			735.41	43.99	735.41	22.38				
722.0	1.96E-04	Am-241			779.73	26.76	792.40	16.96	735.41	16.13	733.83	3.69
756.4	3.47E-06	Pu-239	778.33		838.30	42.20	847.80	27.65	779.73	14.10	781.32	3.13
843.78	1.34E-07	Pu-239	846.79, *836.6	1120, *103	879.45	18.34	895.28	16.12	846.21	16.99	852.54	4.47
898.1	1.80E-08	Pu-239	881.68									
957.6	2.70E-08	Pu-239	*965.49	3.08E+01	963.34	18.86	969.68	19.59	945.93	12.42	945.93	3.53
992.7	3.20E-08	Pu-239	*1005.55, 1014.71	*105, 85.1								
1057.3	4.50E-08	Pu-239	*1079.48, *1092.07, *1099.66	1.73, 15.3, 20.7	1020.30	15.20	1031.40	15.00			1031.40	2.89
		Pu-239	*1172.09	7.59E+00	1121.60	18.53	1118.50	12.70			1135.90	2.96
		Pu-239	*1238.58	1.70E+02	1192.00	17.98						
					1244.80	12.52					1239.90	2.52
1333		(n,γ)**	1332.6	291	1312.90	22.34			1320.50	11.76	1326.70	3.03
					1367.50	12.11						
1434		(n,γ)**	1433.65	420	1419.30	28.24	1422.40	13.34	1414.50	12.36	1427.10	3.58
1454		(n,γ)**	1453.94	377	1469.70	16.60						
			*1530.57, *1568.68	44.8, 17.3	1561.10	12.61	1598.90	10.71			1679.30	2.24
			*1704	3.92E+00			1682.40	12.77				
			*1807.07	8.57E+01			1781.70	11.69				
			1938.07	1.82E+01	2049.60	13.88						
					2182.00	18.21						
2223		H(n,γ)	*2213.46	1.11E+02	2278.10	13.34					2246.60	2.10
			*2307.27	7.13E+00								
			*2527.85	1.20E+01								
			*2644.9	2.19E+01								
			*2750.68	3.39E-01								
			*2961.84	4.78E+02								

Table. 3. Ratios of Key observed WGPu photopeak yields for NaI with ASEDRA and HPGe for standard settings.

Known Pu Energy	HPGe Energy	HPGe Results	ASEDRA Energy (10 Min)	ASEDRA 10 Min	ASEDRA 10 Min Iron DRF	ASEDRA Energy (5 Min)	ASEDRA 5 Min	ASEDRA 5 Min Iron DRF	ASEDRA Energy (1 Min)	ASEDRA 1 Min	ASEDRA 1 Min Iron DRF
333 (w 344)	332.20	0.87	335/ --	1.67 / 1.00							
	0.19/0.13	*OTS Soft.									
344 (w 333/336)	345.00	0.90	-- / 341		1.26 / 0.68	344/345.5	2.05E+00 / 1.10E+00	1.51 / 0.81	347	1.87 / 1.00	1.37 / 0.73
375	374.90	1.00	383/384	1	1	383/384	1	1.00	386	1	1
414	413.60	0.61	417/419	0.74	0.68	420	0.65	0.62	420	0.79	0.79
722/622	722.10	1.26	748	1.28	1.34	733	1.24	1.28			

4.4 Runs with Optimized Settings

Analysis with ASEDRA setting changes including addition of a tailing correction, a higher threshold for higher statistics (10 minute) runs, and higher scale energy and FWHM calibrations. Ratios of observed to predicted yields for key WGPu and Am Lines, normalized to the 375 keV and 414 keV lines, are shown in Table 4 for these optimized settings, also compared to HPGe results. Again, the calculated ratios include corrections for measured detector efficiency, branching ratios, and source shielding, while the MCNP values compare ratios to results from the MCNP transport model with the PuBe source and source shielding, HPGe and NaI detectors. The 344 keV peak includes contributions from the 332/336 keV peaks, while the 375 keV peak includes the contributions of the 380 and 382 keV peaks.

Table. 4. Ratios of WGPu photopeak yields for NaI with ASEDRA and HPGe for standard settings.

Known E (keV)	HPGe 10 Min (375 keV) Calc/MCNP	HPGe 10 Min (414 keV) Calc/MCNP	ASEDRA - NaI 10 Min (375 keV) Calc/MCNP	ASEDRA - NaI 10 Min (414 keV) Calc/MCNP	ASEDRA - NaI 5 Min (375 keV) Calc/MCNP	ASEDRA - NaI 5 Min (414 keV) Calc/MCNP	ASEDRA - NaI 3 Min Poly (375 keV) Calc/MCNP	ASEDRA - NaI 3 Min Poly (414 keV) Calc/MCNP
332	0.87/1.38	0.66/1.19						
*OTS	0.1/0.15	0.07/0.13						
344	0.91/0.81	0.88/0.83	1.0/1.13	1.29/1.21	0.91/1.03	1.30/1.22	1.13/1.28	1.30/1.22
367	0.77/0.44	0.81/0.47	1.75/1.55	2.25/1.66	2.43/2.16	3.45/2.55	2.79/2.47	3.2/2.36
375	1	0.61/1.08	1.00	1.29/1.07	1	1.43/1.18	1	0.54/0.96
414	1.64/0.93	1	0.78/0.93	1	0.70/0.57	1	1.85/1.04	1
662	2.31/0.49	2.19/0.525	1.69/1.16	2.17/1.79	1.62/1.12	2.31/1.9	3.07/2.10	3.51/2.90
722/622	0.785		0.75		0.8		0.58	
511	(To HPGe)		0.694		0.71		0.6	

5. CONCLUSIONS

5.1 Photopeak Yield Comparisons

Close inspection of the results reveals that the analyzed photopeak yield ratios for ASEDRA processed NaI spectra are comparable to HPGe detector results, and in some cases better. In addition, the ratios of key energy lines are in agreement with relative yields predicted by the known branching ratios [4,5]. While not all lower energy Pu lines were analyzed due to possibly high error in attenuation corrections at lower energies, the relative ratios of the key lines in the 300 keV to 400 keV region (332 keV, 345 keV, 375 keV, and 414 keV), and should be most important in a nuclide identification routine.

5.2 Photopeak Analysis

ASEDRA processed NaI spectral results for WGPu give energies identified to within 1 % and one-half of a FWHM with standard settings and calibration, and usually better ($\sim$ 5 keV). ASEDRA smoothing and fitting of NaI spectra produces results comparable to that of a higher resolution detector, with no prior information on the spectra. For side-by-side comparisons, the ASEDRA-processed NaI results showed nearly all of the photopeaks found by the HPGe detector, with the exception of several weaker peaks closely spaced in energy from a more predominant peak. However, some weaker lines were found by NaI-ASEDRA not identified by the HPGe detector; in particular, the 2223 keV H(n,γ) line, and the ~550 keV Ge(n,n') line. The accuracies of photopeak energies are comparable to those from a detector of 1% resolution for runs with good statistics. such as the 10 minute unshielded PuBe run, and or strongest peaks such as the 344, 375, and 414 keV peaks. The accuracy of photopeak energies for lower statistics, such as shorter count times with the shielded source or weaker lines, are comparable to those from a detector of ~2% resolution.

The ASEDRA results from the limiting case for statistics and shielding, the 1 minute run with the composite shielding material are noteworthy; these show the key Pu peaks at 344 keV, 375 keV, and 414 keV, and 452 keV, as well as the 662 keV [241]Am peak. ASEDRA also identifies contaminant photopeaks found in the longer 10 minute HPGe run with the shielded source. There appear to be few false positives, in contrast to the lower threshold shielded HPGe analysis. The WGPu test spectra analyzed in this work show that ASEDRA can enhance peak identification capabilities for lower resolution scintillator detectors such as NaI detectors to a level that is comparable to a higher resolution detectors, such as HPGe.

ASEDRA synthetic resolution and ACHIP noise reduction software packages are now licensed by HSW Technologies LLC (www.hswtech.com, email info@hswtech.com).

REFERENCES

[1] E. Lavigne, G. Sjoden, J. Baciak, and R. Detwiler, "ASEDRA – Advanced Synthetically Enhanced Detector Resolution Algorithm, a code package for post processing enhancement of detector spectra," FINDS Institute, Nuclear and Radiological Engineering Department, University of Florida, (2007).

[2] E. LaVigne, G. Sjoden, J. Baciak and R. Detwiler, "Extraordinary Improvement in Scintillation Detectors Via Post Processing with ASEDRA—Solution to a 50-year-old Problem", Upcoming Presentation / Paper for SPIE Defense and Security Symposium 2008, (March 2008).

[3] G. Ghita, G. Sjoden, J. Baciak, "A Method For Experimental and 3-D Computational Radiation Transport Assessments of PuBe Neutron Sources," Nuclear Technology, Vol 159, (2007).

[4]   Reilly, et al, "Passive Non-Destructive Assay of Nuclear Materials, " NRC, USG, pp. 221-271., (1991)

[5] Korean Atomic Energy Research Institute, Table of Nuclides, http://atom.kaeri.re.kr/.

[6] National Institute of Standards and Technology, http://www.NIST.gov/.